Pramaṇa – J. Phys., Vol. 32, No. 3, March 1989, pp. 209–229. © Printed in India.

Effective decoupling in some odd-A odd-Z rotational bands

KIRAN JAIN*†, A K JAIN* and R K SHELINE

Florida State University, Tallahassee, Florida 32306-3006, USA
*Permanent address: Department of Physics, University of Roorkee, Roorkee 247 667, India

MS received 12 May 1988; revised 7 November 1988

Abstract. A systematic analysis of the results of single quasiparticle-plus-rotor bandmixing calculations is presented wherein the empirically noticed characteristic effective decoupling patterns and their systematics in certain odd-A odd-Z rotational bands based on $h_{9/2}$, $d_{5/2}$, $h_{11/2}$ and $g_{7/2}$ orbitals are reproduced. The strategy adopted allows us to obtain an almost unique set of parameter values for a given decoupling pattern. The composition of wavefunctions in terms of core rotational angular momentum supports the idea of effective decoupling. These wavefunctions are then used to analyse the extent and nature of Coriolis coupling in these bands. It is found that either one or both parts of the Coriolis energies, diagonal and non-diagonal, are significant in most of the cases and the non-diagonal part is mainly responsible for the effective decoupling. These Coriolis effects prominently affect the intraband $B(M1)$ and $B(E2)$ values and their variation with spin is discussed An unusual feature in the $B(M1)$ value of the $h_{9/2}$ orbital based band is pointed out.

Keywords. Nuclear structure; Odd-A odd-Z rotational bands, particle-rotor model; effective decoupling; Coriolis effects; B(E2) and B(M1) values.

PACS Nos 21·10; 21·60

1. Introduction

The odd-A rotational bands in the rare-earth and actinide regions are usually classified into the strongly perturbed bands (SPB) and the strongly coupled bands (SCB). If the energies of the SPB look as if the ground state band of the even-even core nucleus has been superimposed on the bandhead of the odd-A band, it is termed as a decoupled band. In these bands, the strong Coriolis force has effectively 'decoupled' the odd particle. This situation usually arises when deformation is not large and the odd-particle occupies a high-j, low-Ω single particle state (Stephens and Simon 1972; Stephens *et al* 1973; Stephens 1975), the famous example being the $i_{13/2}$ neutron orbital. However, if we dilute our concept of decoupling, we could show that decoupled bands of a generalized nature are not uncommon (Jain and Jain 1984). The new type of decoupled bands represent a partial alignment of the odd-particle which now carries an effective aligned spin j plus a core having its lowest rotational angular momentum $R' = 2$ or 4 or 6 (for the bandhead) instead of the usual $R = 0$ value. Thus we get decoupled bands based on a rotationally excited core. Experimental data on the $i_{13/2}$ orbital-based bands support this picture very well (Jain and Jain 1984). A detailed analysis of the wavefunctions in terms of their R-composition (R is

† To whom all correspondence should be addressed.

the core rotational angular momentum) and the expectation values of R confirm this (Jain 1987). An interesting outcome of this study was the fact that the non-diagonal Coriolis contribution remains quite significant up to almost the top of the $i_{13/2}$ orbital. On the other hand, the diagonal part of the Coriolis force is significant only up to the $\Omega = 5/2$ level of the $i_{13/2}$-orbital and is mainly responsible for the relative shifting of the favoured and the unfavoured sequences of the $i_{13/2}$ band with respect to each other. The relative shifting and therefore the immediate recognition of a band as a decoupled band disappears after the middle of the $i_{13/2}$-orbital, but enough of non-diagonal Coriolis contribution remains to produce what we call an effective decoupling.

It was suggested by one of us (Jain 1984) that many of the rotational bands, usually interpreted as normal bands, may also be looked upon as effectively decoupled bands. The empirical evidence in favour of this interpretation is quite impressive in many cases. As an example, we show in table 1, the transition energies of the five bands known in ^{161}Ho in comparison with the transition energies of the core nucleus ^{160}Dy. The energies have been arranged so that they display best matching with the ^{160}Dy ground band transition energies. Except for the lowest transition energy, which is sometimes quite off, we can see a remarkable closeness in the transition energies which hints at the existence of a decoupling behaviour. We must point out that often only one of the two $\Delta I = 2$ sequences of a given band exhibits this behaviour. However, there are examples, where both the $\Delta I = 2$ sequences exhibit this kind of behaviour.

The usual interpretation of these bands would be in terms of a SCB based on a Nilsson level with Ω as a good quantum number. We can employ the perturbation expansion of Bohr and Mottelson (1975) to fit the energy spectrum of these bands with an expression

Table 1. The transition energies of one of the $\Delta I = 2$ sequences of the strongly coupled bands of ^{161}Ho are compared with the transition energies of the ground state rotational band of ^{160}Dy The transitions of the odd-A nuclei are appropriately displaced for the best matching. $j_{R'} = I - R$ is the effective aligned spin as defined in the text. The data have been mostly taken from the references (Sakai 1984; Table of Isotopes 1978) and a private compilation.

Transition energy ΔE(keV)					
^{160}Dy	^{161}Ho				
Ground band	$1/2^+[411]$ $j_{R'} = 0{\cdot}5$	$1/2^-[541]$ $j_{R'} = 0{\cdot}5$	$7/2^-[523]$ $j_{R'} = 1{\cdot}5$	$3/2^+[411]$ $j_{R'} = -0{\cdot}5$	$7/2^+[404]$ $j_{R'} = 0{\cdot}5$
(2→0)	(5/2→1/2)	(9/2→5/2)			
86·79	105·3	120 5			
			(11/2→7/2)	(7/2→3/2)	
197·0	203·0	208 6	221·9	164·5	
					(13/2→9/2)
297·24	301·5	296 3	312·5	269·2	303 7
385·68	389 8	381·2	397·2	361·1	385 0
461·88	463 5	461·3	472·5		454·4
522·8			534·4		518·7

$$E(I,K) = E_K + A[I(I+1) - K^2] + B[I(I+1) - K^2]^2 + C[I(I+1) - K^2]^3 + \cdots + (-1)^{I+K} \prod_{i=1-K}^{K} (I+i) \times \{A_{2K} + B_{2K}[I(I+1) - K^2] + \cdots\}. \quad (1)$$

This equation can describe a large number of rotational bands with good accuracy. However, it does not provide much physical insight. Moreover, as noted by Bunker and Reich (1971) and also by Ogle *et al* (1971), the Coriolis effects could be quite large in many of these bands e.g. bands based on orbitals originating from $h_{9/2}$ state. Much of the data in most of these nuclei has become available after 1970 and has not been subjected to a systematic analysis. It would therefore be interesting to carry out a systematic analysis to determine the extent and nature of Coriolis effects in these bands and to see whether it leads to what we call an effective decoupling.

The particle-rotor model calculations recently done by Smith and Rickey (1976) in $^{101-105}$Pd, Popli *et al* (1979) in $^{105-107}$Ag, Wohn *et al* (1985) in ^{99}Y and Bhattacharya *et al* (1985) in $N = 88$ isotones have been quite successful in interpreting the band-structure of these nuclei. It is interesting to note that significant Coriolis effects were observed for bands based on orbitals like $g_{7/2}$ and $d_{5/2}$. We may therefore expect that significant Coriolis effects may persist in many of the SCB of the odd-A rare-earth nuclei. Even small rotational effects show up prominently in the transition probabilities particularly the magnetic dipole transitions (Hamamoto 1981). We therefore expect the Coriolis effects to affect the $B(E2)$ and $B(M1)$ values in a significant way.

In the present paper, we present a systematic analysis of the results of a schematic one BCS-quasiparticle plus rotor bandmixing calculations for odd-A odd-Z rotational bands based on orbitals belonging to $h_{9/2}$, $d_{5/2}$, $h_{11/2}$, and $g_{7/2}$ states. Significant Coriolis effects are shown to be present in many of the cases which lead to an effective decoupling pattern. These in turn lead to some interesting features in the $B(M1)$ and $B(E2)$ values.

We have completely refrained from including any modifications in the particle rotor model as are now available in the literature (Smith and Rickey 1976; Rekstad and Engeland 1980; Muller and Neergard 1983; Engeland *et al* 1983; Muller and Mosel 1984). All the newer versions have their limitations in terms of applicability and ease of handling. It remains a fact that the simplest version of the particle-rotor model is still best suited for global studies and fits in very easily in the strategy outlined below and adopted by us. Besides, it has the advantage of a minimum number of parameters, avoids the uncertainties involved in introducing any new factors and has a great deal of transparency to reveal the underlying physics.

In §2, we present the models and the methodology used in the calculations. In §3, we discuss the results of our calculations and present the conclusions in §4.

2. Models and the methodology

We have used the standard particle-rotor model as described earlier (Jain and Jain 1984; Jain 1987). However, we give the important expressions for completeness. The total Hamiltonian of the system is

$$H = H_{\text{s p}} + H_{\text{rot}} + H_{\text{cor}}, \tag{2}$$

where $H_{\text{s.p.}}$ is the single particle deformed shell model Hamiltonian (in our case the Nilsson model) and

$$H_{\text{rot}} = \frac{\hbar^2}{2\mathscr{I}}[I^2 + j^2 - I_z j_z], \tag{3}$$

$$H_{\text{cor}} = -\frac{\hbar^2}{2\mathscr{I}}[I_+ J_- + I_- J_+] \tag{4}$$

with the terms having their usual meaning. The basis functions used are the conventional wavefunctions for an axially symmetric rotor given by

$$|IMK\rangle = \left(\frac{2I+1}{16\pi^2}\right)^{1/2}[D^I_{MK}\chi_K + (-1)^{I+K}D^I_{M,-K}R_i\chi_K], \tag{5}$$

where $R_i = \exp(-i\pi J_y)$, represents a rotation of π about the y-axis and

$$\chi_K = \sum_j C_{jK}|j, K\rangle \tag{6}$$

are the eigenfunctions of the Nilsson model Hamiltonian. The diagonalization of H leads to Coriolis mixed eigenfunctions

$$|IM\rangle = \sum_K f_{IK}|IMK\rangle, \tag{7}$$

where f_{IK} are the expansion coefficients. In order to identify the rotational composition of the final state $|IM\rangle$, we expand them in terms of states with good R and j where R is the rotational angular momentum of the core, so that

$$|IM\rangle = \sum_{jR}\sum_K f_{IK}\alpha^{(K)}_{jR}|IMjR\rangle, \tag{8}$$

where

$$\alpha^{(K)}_{jR} = \sqrt{2}\langle IKj - K|R_0 0\rangle(-1)^{j-K}C_{jK}. \tag{9}$$

The fraction of the state $|IM\rangle$ which contains $R = R_0$ is then given by

$$P(IM, R_0) = \sum_j \langle IMjR_0|IM\rangle^2 = \sum_j\left(\sum_K f_{IK}\alpha^{(K)}_{jR_0}\right)^2 \tag{10}$$

For a given level, we also calculate the expectation value $\langle R\rangle$ as

$$\langle R\rangle = \sum_R P(IM, R)[R(R+1)]^{1/2}. \tag{11}$$

The single particle energies e_K, which are eigenvalues of the Nilsson model Hamiltonian, were transformed into quasiparticle energy E_K according to

$$E_K = [(e_K - \lambda)^2 + \Delta^2]^{1/2} - \Delta, \tag{12}$$

where λ is the Fermi level energy and Δ the pairing gap energy.

As pointed out in the introduction, many SCBs can also be looked upon as effectively decoupled bands. The strategy adopted in this paper is therefore to first identify the characteristic decoupling patterns displayed by the experimentally known rotational bands. For example, if we find that a given band displays a decoupling pattern wherein the lowest transition ($9/2 \rightarrow 5/2$) corresponds to ($2 \rightarrow 0$) transition and so on, it implies assigning R-values $0, 2, 4, \ldots$, to $I = 5/2, 9/2, 13/2, \ldots$, respectively. In order to check the validity of this assignment and the reproduction of these bands by theory, we have made a detailed analysis of the results obtained from the rotor-BCS quasiparticle bandmixing calculations. The two important criteria used by us are the analysis of transition energy patterns and the wavefunctions.

Firstly, we analyse the energies. We choose the lowest level energy $E(I_0)$ as the reference level and calculate the ratios $\Gamma(I) = (E(I) - E(I_0))/(E(I_0 + 2) - E(I_0))$ for the sequence of levels $I = I_0 + 2, I_0 + 4, \ldots$, etc by using the calculated level energies. If the assigned R-values are $R = 0, 2, 4, \ldots$, for the levels $I = I_0, I_0 + 2, I_0 + 4 \ldots$ respectively, as in the example quoted above then a calculation of the ratios $\Gamma(I)$ is equivalent to calculating the ratios $(E(R) - E(0)/(E(2) - E(0))$. Provided the calculated band is an $R = 0$ type decoupled band, these ratios should come just close to the set of values, 1, 3·3, 7, 12,..., etc. for $I = I_0 + 2, I_0 + 4, \ldots$, etc. respectively. It should be noted that we compare $\Gamma(I)$'s with the ratios of the energies of a rigid-rotor. This is because we have used a constant moment of inertia parameter and therefore feel that a rigid-rotor band must be used as the even-even core band. Similarly if the decoupled band expected is of the type $R = 2, 4, 6, \ldots$ etc. or, $R = 4, 6, 8, \ldots$ etc. for $I = I_0, I_0 + 2, I_0 + 4, \ldots$ etc. then the set of values obtained for the ratio $\Gamma(I)$ should be close to (1, 2·57, 4·7, 7·4,..., etc.) or, $(1, 2{\cdot}36, 4{\cdot}09, 6{\cdot}18, \ldots$ etc.) respectively. It is thus clearly possible to identify the type of decoupling pattern that the calculated band exhibits. Further, since only ratios are being compared, the assignment of R-values to I-values of a band is almost independent of the input moment of inertia parameter. In our picture, the total angular momentum $I = R + j_{R'}$ where R is an effective rotational angular momentum of core and $j_{R'}$ is an effective aligned spin.

The second criterion to test the association of R-values with the I-values of a band is to consider the average value of $\langle R \rangle$ calculated from the wavefunctions transformed to R-basis and the R-composition of the wavefunction. Since R is not a good quantum number we expect that the average value of R should match reasonably well with the assigned value. However, we do not expect even a reasonable matching for the lowest of the states because in many cases the experimental data indicate very poor matching for the lowest transition energy. Calculations also reveal that the Coriolis energy is very small for lowest state and therefore we do not expect significant alignment for the lowest of spins.

The parameters used in the calculations are the deformation of the nucleus, the pairing gap, the moment of inertia and the Coriolis multiplication factor κ. The deformation parameters used are indicated in the figures which display the results of our calculations and represent the typical values in the rare-earth region. The variation in deformation in a given isotonic chain has been taken into account. A constant value of the input moment of inertia parameter $\hbar^2/2\mathscr{I} = 13\,\text{keV}$ and also the pairing gap parameter $\Delta = 1\,\text{MeV}$ was used. Small changes in these parameters do not significantly affect the outcome of our results. The Fermi energy has been used as a parameter to reproduce the systematics of bands originating from a given type of orbital (say $h_{9/2}$). Since we are not trying to reproduce the band structure of any

given nucleus, different locations of Fermi energy for the same nucleus has no effect on the outcome of our study. We nowhere compare the absolute locations of different bands with respect to each other in a single nucleus. Such an exercise will require, besides locating the Fermi energy of a nucleus, consideration of many other factors and is not the aim of our study. Besides Fermi energy, the only parameter which can be varied with a little freedom is the Coriolis multiplication factor κ.

The single particle basis and energies were obtained from a Nilsson model calculation (Chi 1966; Lamm 1969). The recoil term was also included (but not the many-body recoil contribution) in our calculations. We find that almost a unique set of parameters were required to reproduce the characteristic decoupling pattern observed in the empirical data and that the Fermi energy required to be varied smoothly with Z to reproduce the systematics. The wavefunctions so obtained were then analysed for their R-composition and the average value of R to see the nature of decoupling. Also, we have used these wavefunctions to calculate the transition properties like $B(E2)$ and $B(M1)$ values (Chi 1966; Brockmeier *et al* 1965; Browne and Femenia 1971). We also analyse the diagonal and the nondiagonal parts of the Coriolis energies which shed light on the emergence of the effective decoupling pattern.

3. Results and discussion

3.1 $h_{9/2}$ *orbital based bands*

We present the results of our calculation in figures 1–5 for the bands usually assigned the Nilsson quantum numbers as $1/2^-[541]$ belonging to the $h_{9/2}$ orbital. In the lower part of figure 1 we present the experimental data on these bands in comparison to the transition energies of the ground rotational band of respective core. In most of the cases the transition $(9/2 \rightarrow 5/2)$ corresponds to the $(2 \rightarrow 0)$ transition of the core band. In most cases, the correspondence is quite impressive. Note that the $I = 1/2$ level in most of the nuclei lies lowest and very close to the 5/2 level, and is not shown in the figure. In ^{185}Ir, $I = 5/2$ level lies lowest and close to the 9/2 level. Our calculations reproduce these levels correctly although not shown in the figure. Also, we consider only one of the two $\Delta I = 2$ sequences because it exhibits the best decoupling pattern. The general trends of the other sequence not shown in the figure are also reproduced by our calculations.

Results of our calculation are shown in the upper part of figure 1. The overall trend and systematics can be accounted for as we move from $Z = 67$ to $Z = 77$ by a slight rise in the Fermi energy from a little below the $|\Omega = 1/2\rangle$ to a little above the $|\Omega = 1/2\rangle$ level. Also, the deformation decreases from $\delta = 0{\cdot}27$ to $\delta = 0{\cdot}23$ with increase in the proton number. It is interesting to note that $\kappa = 1.0$ in all the cases, i.e. no attenuation is needed. In figure 2 we show the extent and variation of Coriolis energies $E_C^{(I)} = \langle \psi_I^* | H_C | \psi_I \rangle$ for all the five cases considered in figure 1. We have plotted the non-diagonal (dashed lines) and the diagonal $K = 1/2$ (solid lines) contributions separately. The values have been normalized by dividing them by spin I. In going from case 1 to case 5 of figure 1, we find a decrease in the magnitude of the diagonal contribution of the Coriolis energy while, the non-diagonal contribution does not change much. We also notice a small staggering in the non-diagonal part of the Coriolis energy which has an exactly opposite phase to that of the diagonal Coriolis energy. The strong fluctuation in the diagonal Coriolis energy leads to a $\Delta I = 2$ effect

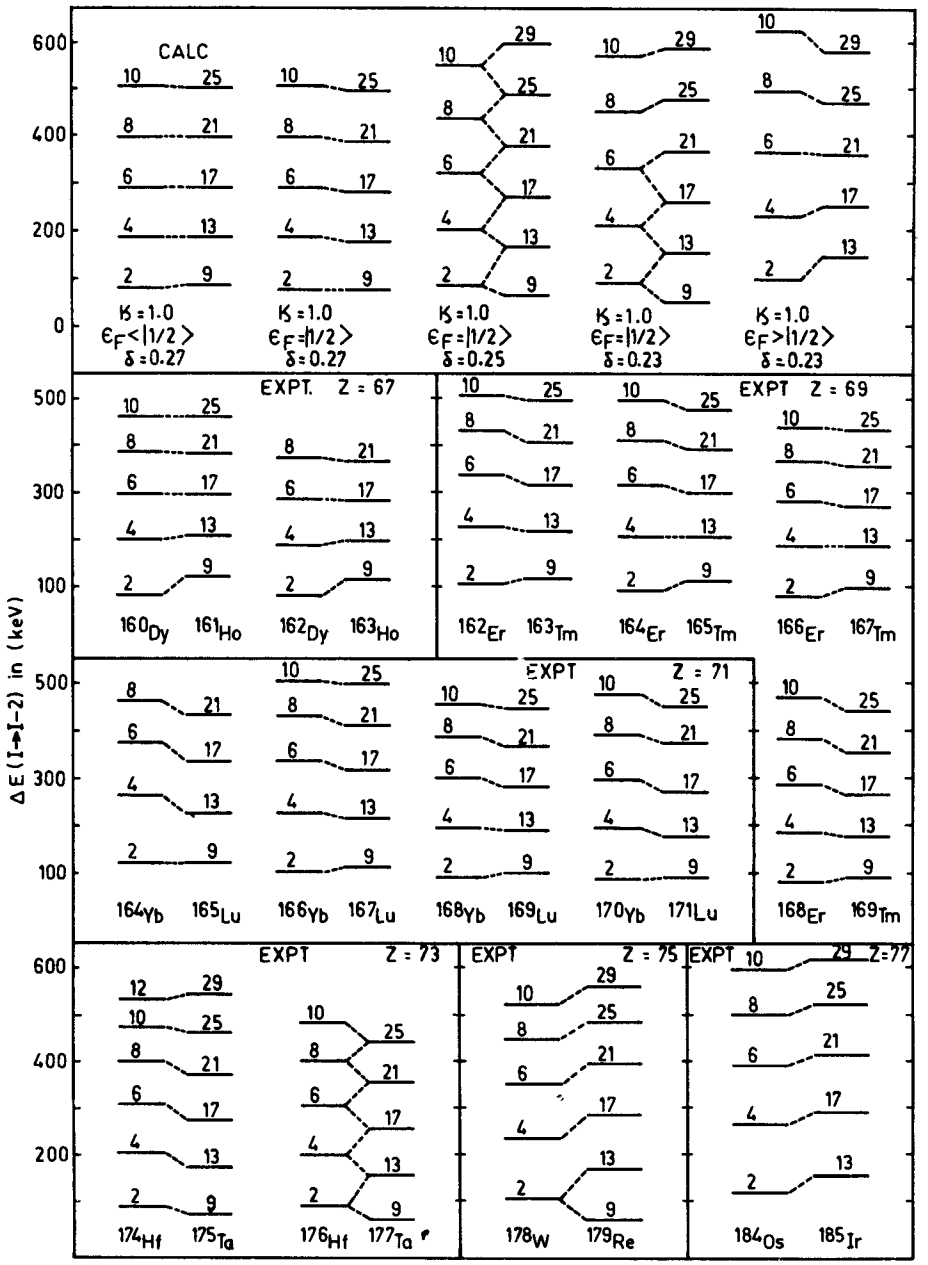

Figure 1. Comparison of the empirical transition energies of odd-A bands with their respective core transition energies displaying the existence of the effective decoupling The odd-A bands are usually assigned the Nilsson configuration $1/2^-[541]$, and in our calculations (top) the Fermi energy indeed lies near this single particle state. The odd-A levels are labelled by 2I The data have been taken from references (Sakai 1984; Table of isotopes 1978) and a private compilation. Here and in the subsequent figures, κ is a factor multiplied to non-diagonal Coriolis matrix element.

in the $1/2^-[541]$ band and the unfavoured sequence is strongly shifted as compared to the favoured one. The magnitude of the Coriolis energies is about two-third of

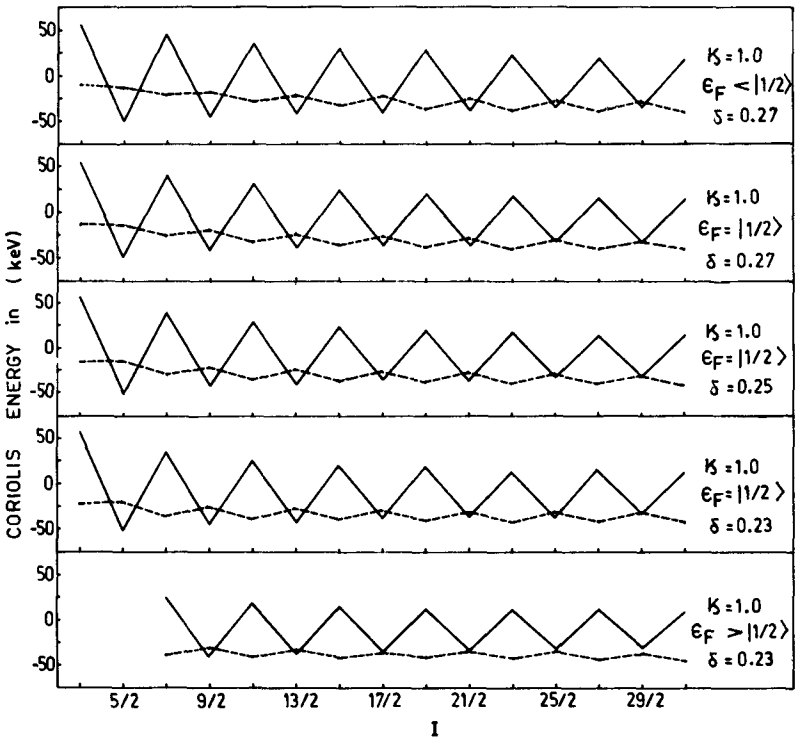

Figure 2. Systematics of the Coriolis energies for the same set of parameters as in figure 1 the diagonal (solid lines) and the non-diagonal (dashed lines) parts These energies have been normalized by dividing them by spin I.

that calculated in similar circumstances for the $i_{13/2}$ neutron band (Chi 1966). Although, the values of Coriolis energy have been normalized by a division of angular momentum I, we can notice a weak spin dependence in both the plotted quantities. In particular the non-diagonal contribution shows a rise with increasing spin while the opposite is true for the diagonal term.

The average value of the core rotational angular momentum $\langle R \rangle$ as calculated from the wavefunction matches exactly with the R-values assigned by us on the basis of the energy systematics (except for the lowest one or two levels). The contribution in the $|IMjR\rangle$ from the assigned value of R and one lower than this, $(R-2)$, is found to vary between 55% to 80% (in going from lower to higher spins).

The intraband transition properties are also calculated for these five cases and shown in figures 3 and 4. Figure 3 contains the results of reduced magnetic dipole transition probability, $B(M1)$ plotted as a function of spin I. Strong rotational effects are seen which decrease marginally while going from case 1 to case 5. The staggering observed here can be directly correlated with the staggering in diagonal Coriolis energy shown in figure 2. A small decrease in the magnitude and the staggering of the diagonal Coriolis energy in going from case 1 to case 5 is reflected dramatically in the $B(M1)$ values. We find the $B(M1)$ values of the transitions $I = j + 2n \rightarrow j + 2n - 1$ (defined as type B transitions by Hamamoto, 1981) almost vanish for the cases 2, 3, and 4 of figure 1. In general we find that the transitions defined as type B are much weaker compared to the type A transitions given by $I = j + 2n + 1 \rightarrow j + 2n$. This trend

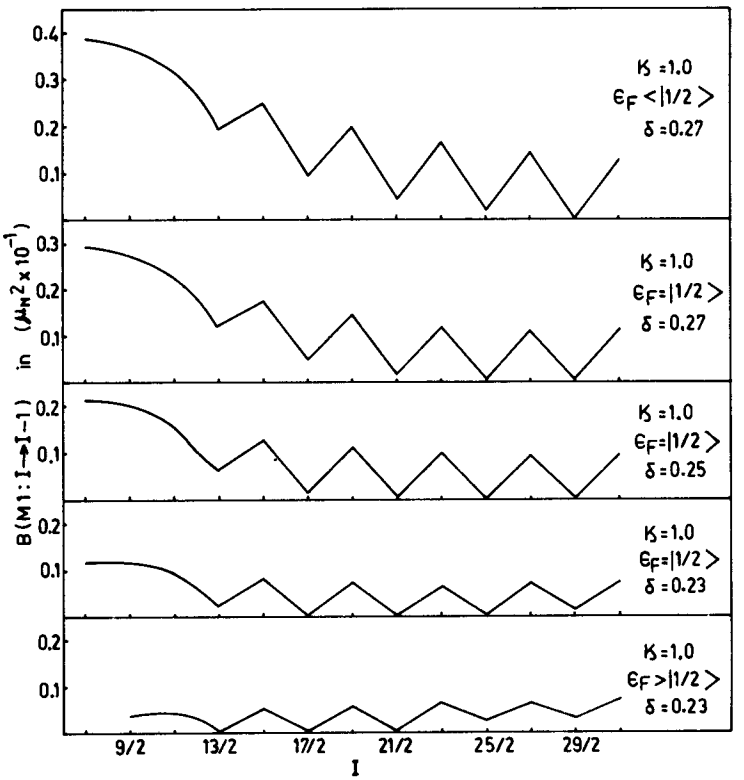

Figure 3. Plots of $B(M1{:}I \rightarrow I-1)$ values for the same set of parameters as in figure 1. The gyromagnetic ratios used are: $g_l = 1$, $g_R = 0{\cdot}43$ and $g_s = 3{\cdot}351$.

is just opposite to that obtained for $i_{13/2}$ odd-neutron bands (Hamamoto 1981; Jain 1987). Moreover, in the case of $i_{13/2}$ bands, a complete vanishing of $B(M1)$ values was obtained for the location of the Fermi energy near $\Omega = 5/2$ level, whereas it is obtained here for $\Omega = 1/2$. In figure 5, we display the experimental transition energies of the $1/2^-[541]$ band corresponding to ^{167}Lu. Along with the spin I of the transition $(I \rightarrow I-2)$ we have also labelled the levels by the R value assigned in the effective decoupling picture. On the right of the experimental data, we have plotted the results of our schematic calculations. Each state I gets a dominant contribution from the core rotation given in the figure and the average value $\langle R \rangle$ also matches closely with this value. We have shown the type A transitions by dashed lines and the type B transitions by solid lines. As already noted above, the type A transitions here are strong and involve a change in the core rotational angular momentum of $\Delta R = 2$, whereas type B transitions are weak and involve a change in the core angular momentum $\Delta R = 0$. Thus the usual explanation offered in the case of $i_{13/2}$-bands that type B transitions should be strong as it involves $\Delta R = 0$, fails (Mosel 1986; Jain 1987). No experimental data are available to us to confirm these results and it would be interesting to verify these results.

In figure 4, we summarize the results of $B(E2)$ for both $\Delta I = 1$ as well as $\Delta I = 2$ transitions. The results are expressed in the units of unperturbed values obtained for $\Omega = 1/2$, a practice adopted by Hamamoto (1981). The $B(E2{:}\Delta I = 1)$ values are

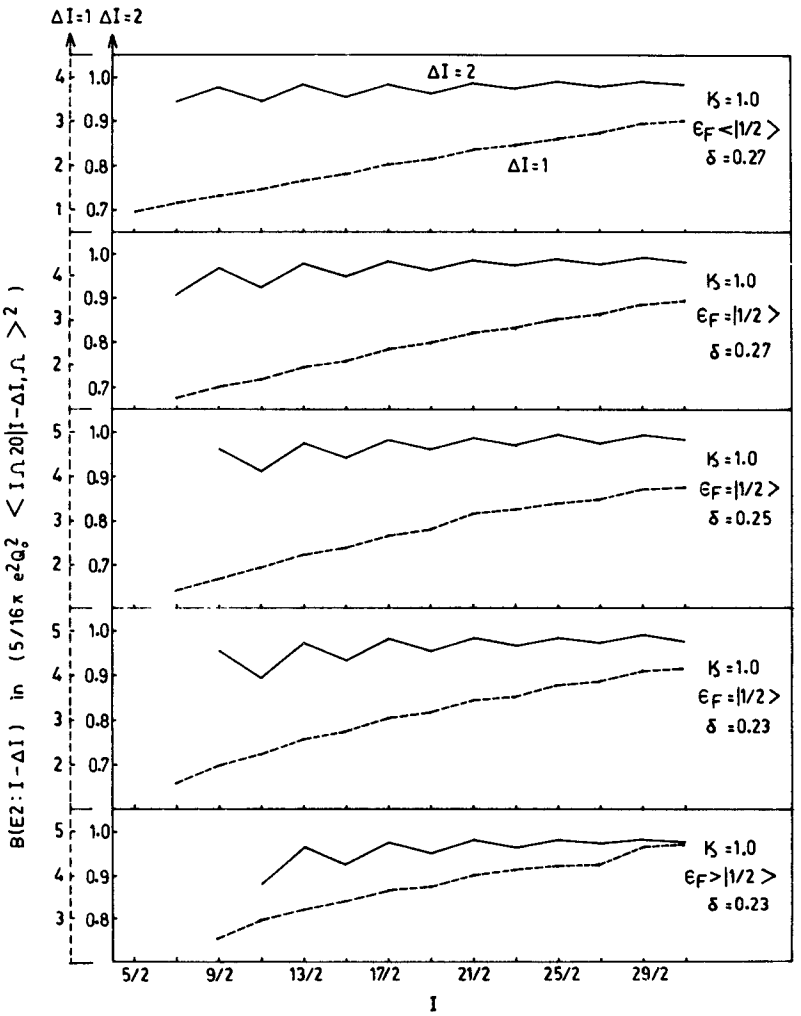

Figure 4. Plots of $B(E2\ I \rightarrow I - \Delta I)$ for all the cases and the same set of parameters as in figure 1

observed to be larger than unity in all the five cases. Since the Fermi energy is near $\Omega = 1/2$ level, this result is very similar to that obtained for odd-neutron $i_{13/2}$ band (Brockmeier *et al* 1965). The $B(E2{:}\Delta I = 2)$ values are always a little less than unity and exhibit a strong staggering effect. It is interesting to note that while the staggering in $B(E2)$ values decreases with increasing spin, it increases in $B(M1)$ values. This is because the magnetic effects increase with rotation.

3.2 $d_{5/2}$ *orbital based bands*

In figure 6, we present the results of our calculation as also the experimental data on the bands supposedly identified as $3/2^+[411]$ and $5/2^+[402]$ bands belonging to the $d_{5/2}$ orbital. It is clear from the comparison of the experimental transition energies with those of the respective core transition energies that there are two distinct types

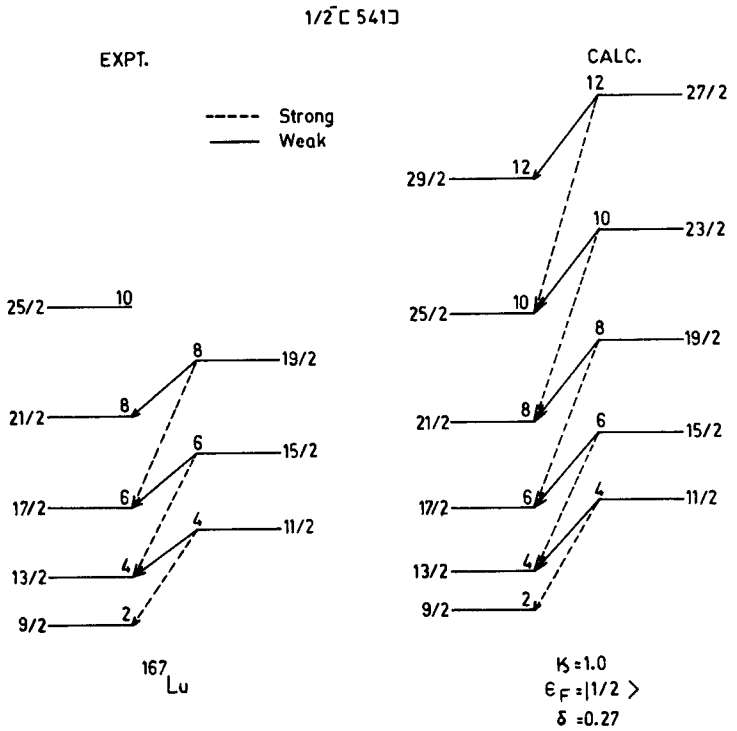

Figure 5. Comparison of the experimental [^{167}Lu] and the theoretical systematics of the 1/2⁻[541] band. The R values have been assigned as in the effective decoupling picture. Type A transitions (dashed) are stronger and involve a change in the core rotation $\Delta R = 2$.

of bands: one in which the $(7/2 \rightarrow 3/2)$ transition of the band corresponds to $(4 \rightarrow 2)$ transition of the core and so on and the other in which the $(11/2 \rightarrow 7/2)$ transition of the band corresponds to the $(6 \rightarrow 4)$ transition of the core and so on. These characteristic band patterns can be reproduced for the set of parameters shown in the figure. As we go from $Z = 67$ to $Z = 75$, the Fermi energy is expected to rise and the deformation is expected to decrease. These facts have been kept in mind while looking for suitable parameter values. Notice that the Coriolis factor $\kappa = 1{\cdot}5$ i.e. we require an enhancement rather than attenuation. It was also pointed out by Bohr and Mottelson (1975) that κ can be greater than unity for certain bands. An analysis of the Coriolis energies, both diagonal and non-diagonal parts, is shown in figure 7. The diagonal Coriolis energy is significant when the Fermi energy is near the $\Omega = |3/2\rangle$ level. However, the non-diagonal Coriolis contribution remains significant for a band based on orbital with j as low as 5/2. It is the non-diagonal contribution which is responsible for the effective decoupling. We point out that in all our discussion we have left the other $\Delta I = 2$ sequence which does not show good effective decoupling pattern. The average value of $\langle R \rangle$ as calculated from the wavefunctions is found to be consistently less by $1\hbar$ as compared to the assigned R-value. The combined contribution from the two R-states, $|R\rangle$ and $|R-2\rangle$, is found to be about 75% to 80% which is quite satisfactory. The wavefunction thus nearly conforms to the assignments of R made by us.

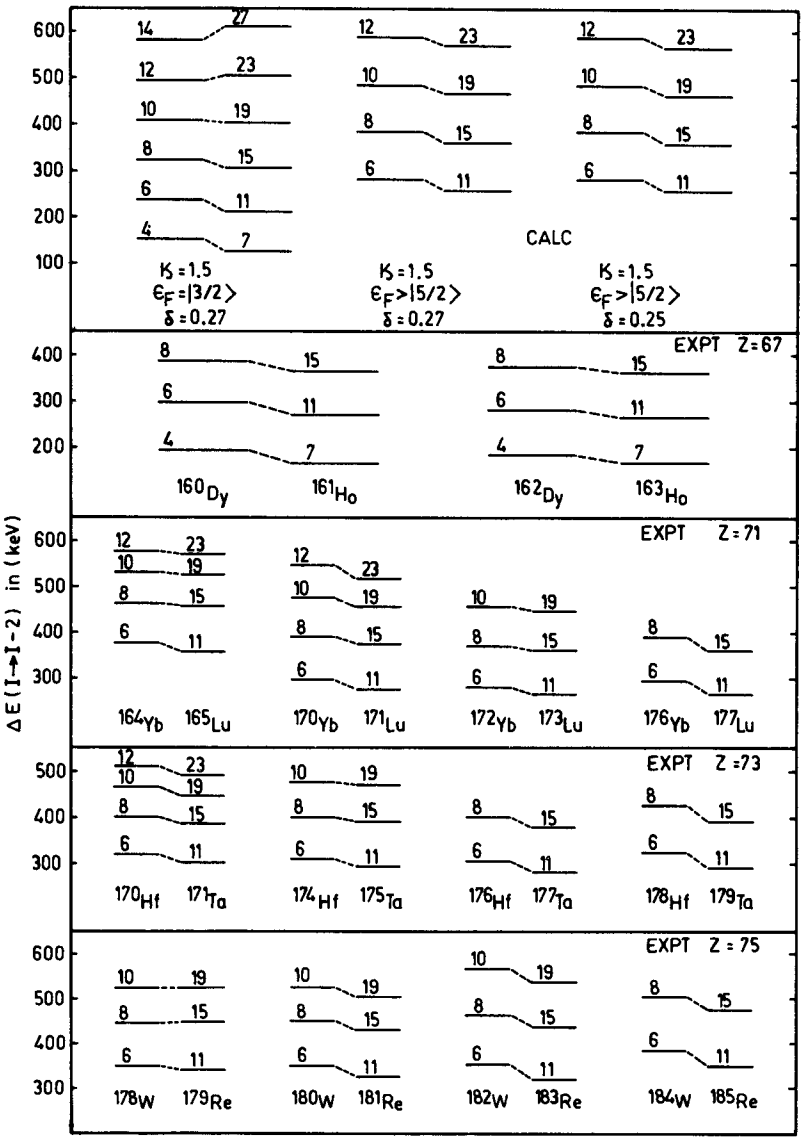

Figure 6. Similar to figure 1 but for the Fermi energy located near the $\Omega = 3/2$ and 5/2 levels of $d_{5/2}$ orbital. Usual band quantum numbers are $3/2^+[411]$ and $5/2^+[402]$

The behaviour of $B(M1)$ values is shown in figure 8. The small fluctuations seen in the diagonal Coriolis energy of case 1 of figure 7 are amplified considerably in the $B(M1)$ values. Very weak staggering effect may be seen at high spins for the rest of the two cases. However, no Coriolis effects were seen in the $B(E2)$ values both for the $\Delta I = 2$ and the $\Delta I = 1$ transitions, which nearly followed the unperturbed rotation values.

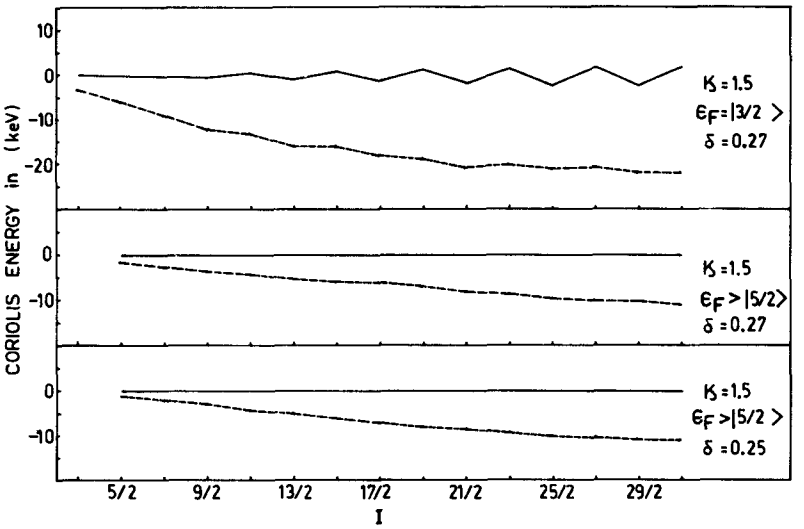

Figure 7. Similar to figure 2 but for the same set of parameters as in figure 6.

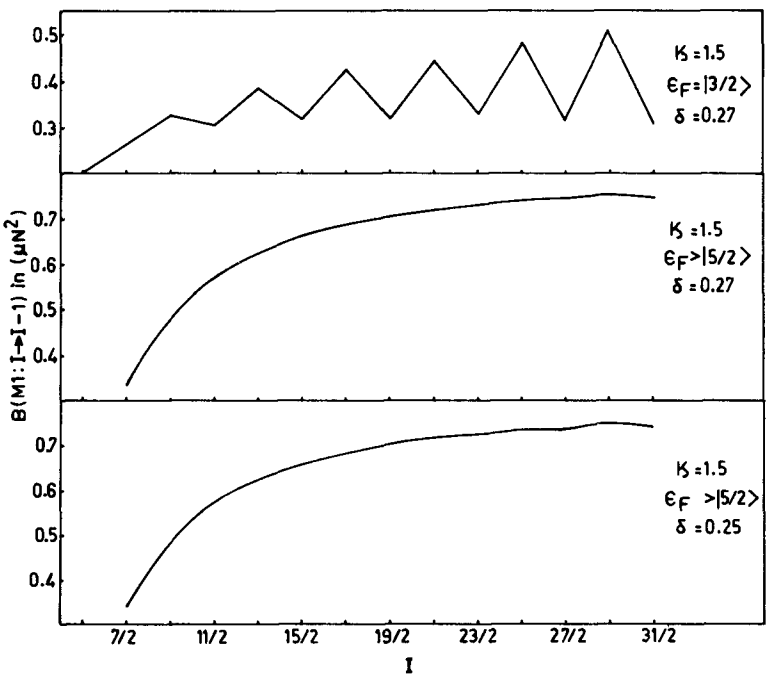

Figure 8. Plots of $B(M1\ I \rightarrow I-1)$ values for the same sets of parameters as in figure 6 The gyromagnetic ratios used are the same as in figure 3.

3.3 $h_{11/2}$ *orbital based bands*

Similar results are displayed in figures 9–12 for bands based on $h_{11/2}$ orbital. These bands are designated by the Nilsson quantum number $7/2^-[523]$ and $9/2^-[514]$.

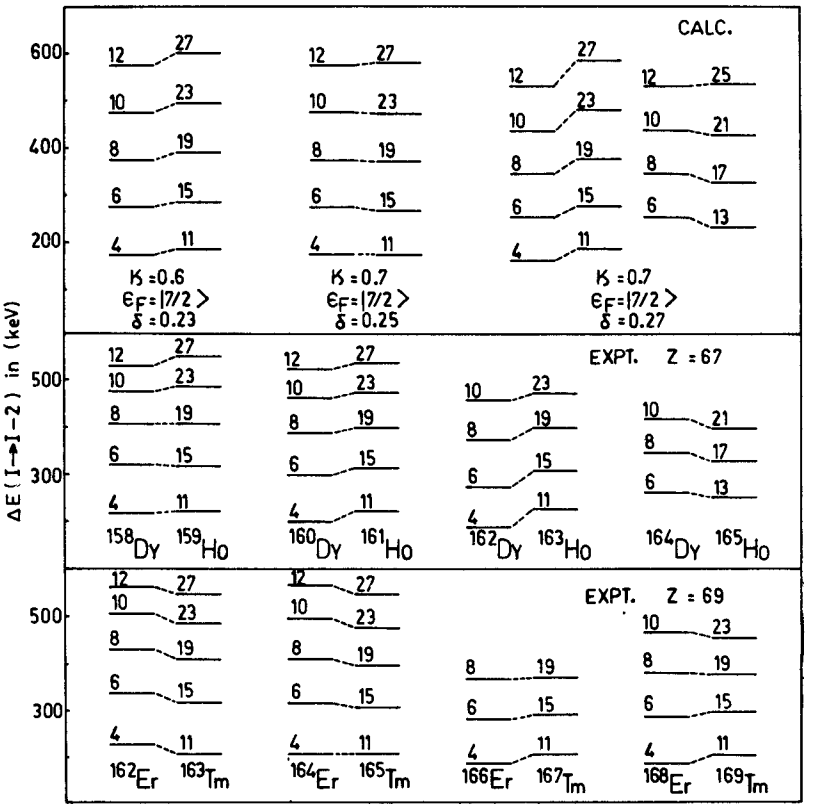

Figure 9. Similar to figure 1 but for the Fermi energy near the $7/2^-[523]$ Nilsson state which belongs to $h_{11/2}$ orbital.

The kind of effective decoupling picture observed in these bands is shown in figures 9 and 10. The correspondence is very good in most of the cases. Note that again only one of the two $\Delta I = 2$ sequences is shown; the other sequence is not so good in most of the cases except for ^{167}Lu and ^{163}Lu shown in figure 10. These characteristic decoupling patterns can be reproduced by the calculations as shown in the upper part of the figure. While the diagonal Coriolis energies in all the cases are zero, the non-diagonal contribution is significant and rises quickly with increasing spins (figure 11). We therefore expect much better decoupling at higher spins. This is clearly reflected in the trends shown by the experimental data (Jain 1984). It may be noted that the Coriolis attenuation factor is taken to be less than unity in calculations.

The calculated R-values are always 1 to 1·5 unit less than the assigned R-values. Also, only about 50% strength is concentrated in $|R\rangle$ and $|R-2\rangle$. Thus in terms of the wavefunctions, the $h_{11/2}$ orbital based bands are not so well decoupled.

The behaviour of $B(M1)$ and $B(E2)$ values is shown in figure 12. We notice that a small staggering in the $B(M1)$ values is present at higher spins when the Fermi energy is near the $\Omega = 7/2$ level, but it completely disappears on raising the Fermi energy to $\Omega = 9/2$. This implies that the staggering effect recently seen in $9/2^-[514]$ band of ^{165}Lu and ^{157}Ho at lower spins (Hagemann *et al* 1984; Jonsson *et al* 1984) must be due to a still lower location of the Fermi energy or a mixing of other $K = 1/2$ level. If we place the Fermi energy somewhere between 5/2 and 7/2 such a staggering is obtained.

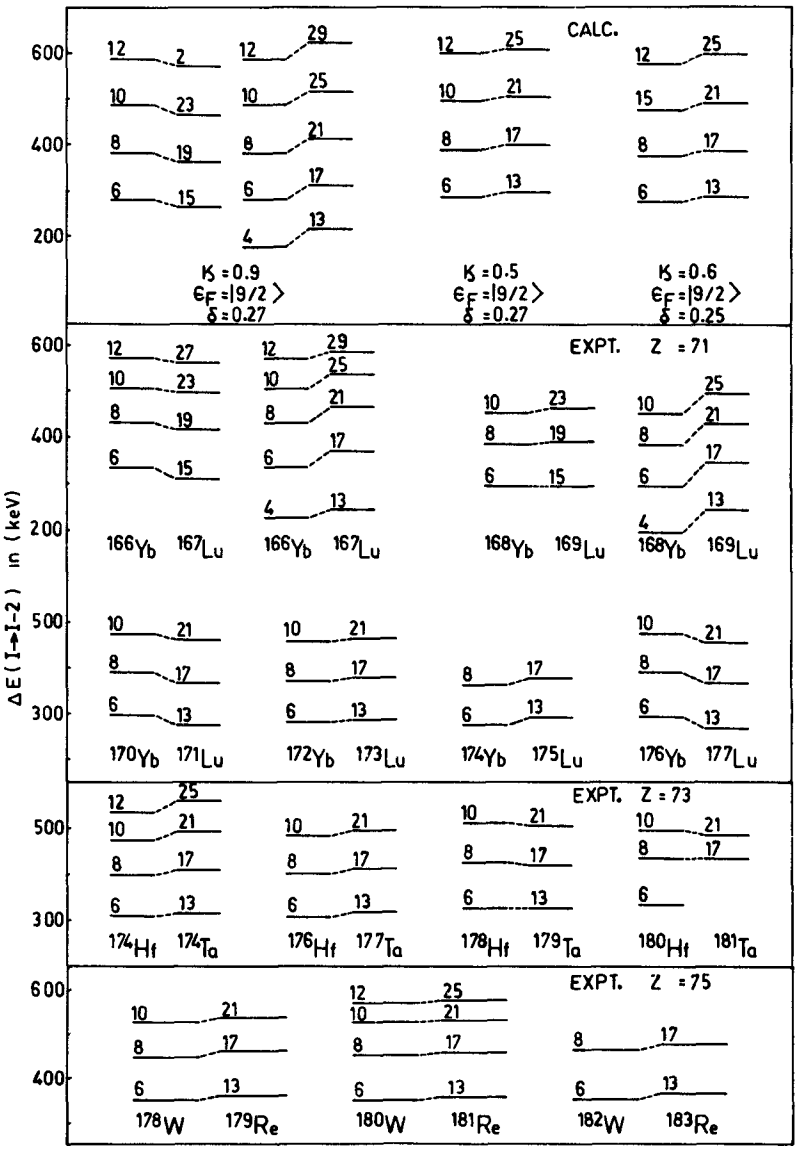

Figure 10. Similar to figure 9 but for the Fermi energy near the $9/2^-[514]$ Nilsson state.

3·4 $g_{7/2}$ orbital based bands

Results for bands based on the $g_{7/2}$ orbital and identified as $7/2^+[404]$ are presented in figures 13(a) and 13(b). Most of the examples again display an effective decoupling pattern wherein the (13/2→9/2) transition corresponds to the (6→4) transition of the core and so on. Here, both the $\Delta I = 2$ sequences have been considered. Figure 13(a) presents the results of $I = j + 2n + 1 \rightarrow j + 2n - 1$ sequence. The Fermi energy is almost at the top of the $g_{7/2}$ orbital and therefore we expect a small Coriolis energy. As shown in figure 14, the diagonal Coriolis energy is zero while the non-diagonal contribution is about 20 keV or more at higher spins. These bands represent examples

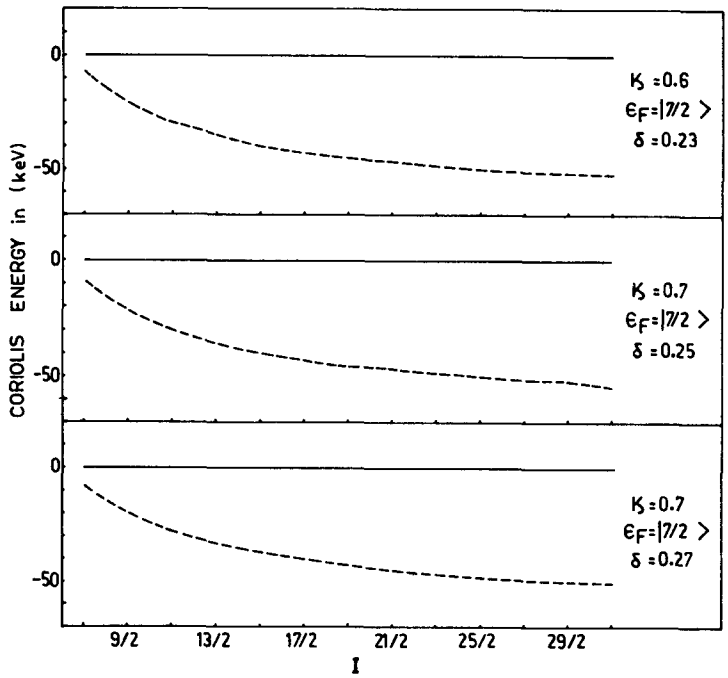

Figure 11. Similar to figure 2 but the same set of parameters as in figure 9. Similar results are obtained for parameters of figure 10 except for a slight decrease in the Coriolis energy.

of bands where the transition $(6 \rightarrow 4)$ corresponds to $(13/2 \rightarrow 9/2)$, and it seems as if the odd-proton spin-1/2 is antialigned to a core of bandhead having a rotational angular momentum $R = 4$.

The analysis of the wavefunction for its R-composition confirms the assignments made by us. Thus, about 97% strength is concentrated in two R-states, one the assigned $|R\rangle$ and another $|R-2\rangle$. Also the average value of $\langle R\rangle$ differs from the assigned R-value by less than $1\hbar$.

4. Conclusions

We have carried out a systematic analysis of the effective decoupling patterns as displayed by some of the experimentally known odd-A odd-Z rotational bands by an application of the traditional particle-rotor model calculations. We point out here that the traditional $\Delta I = 1$ SCB are broken up into two $\Delta I = 2$ bands and often only one of these two exhibits a better effective decoupling. Having identified the characteristic patterns, we proceeded to obtain the set of parameter values which will reproduce these patterns. Remaining within physical limits, we found that this set is almost always unique for a given type of pattern. The resulting wavefunctions were then analysed for their R-composition and the average value of $\langle R\rangle$ to confirm the assignments made by us. Except for the $h_{11/2}$ orbital based bands, we found very good agreement in all cases. We then used these physically meaningful wavefunctions to calculate the Coriolis energies, diagonal and non-diagonal, and the $B(M1)$ and $B(E2)$ values.

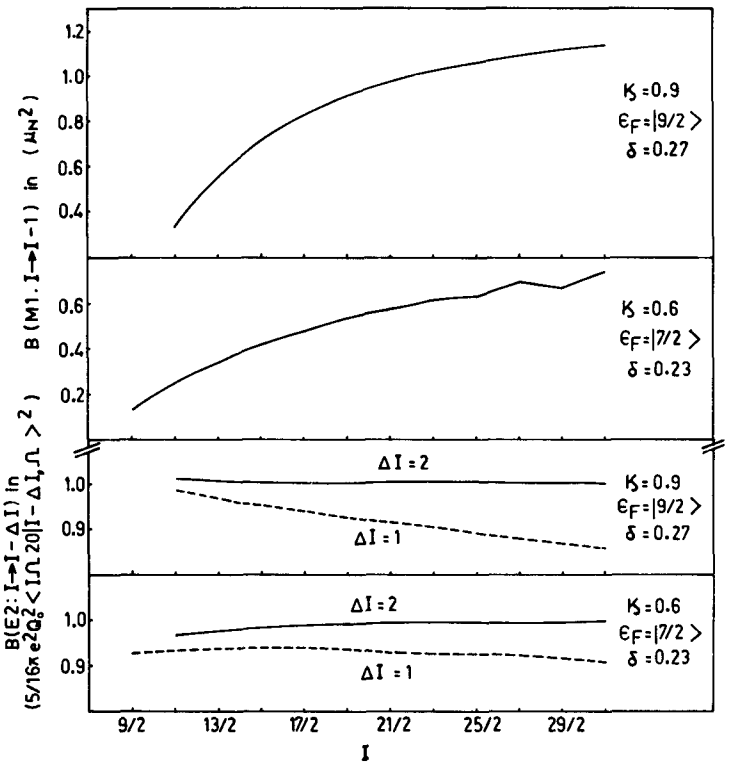

Figure 12. Plots of $B(M1:I \to I-1)$ and $B(E2:I \to I-\Delta I)$ values for the Fermi energy near each of the plots. The gyromagnetic ratios used are same as in figure 3.

It is clear from our results that the $\Delta I = 2$ pattern of some odd-A bands is primarily due to the diagonal part of the Coriolis energy. This is large when the Fermi energy lies near the $\Omega = 1/2$ or $3/2$ single particle levels and leads to the upward shifting of one of the two $\Delta I = 2$ sequences. The absence of the diagonal contribution however does not imply that the degree of decoupling is zero. We have found that the non-diagonal part of the Coriolis energy remains significant even when the Fermi energy is close to the top level of any given orbital. It is this term that leads to the effective decoupling. The increment in this term with increasing spins implies that the degree of effective decoupling becomes much better at higher spins, a fact also evident from the experimental data that we have presented.

The Coriolis effects are seen to have significant effect on the $B(M1)$ and $B(E2)$ transition probabilities within a band. As pointed out by us, the $B(M1)$ values are more sensitive to rotational effects particularly the diagonal part of the Coriolis energy. In the $h_{9/2}$ based bands, the $B(M1)$ values display a behaviour which is quite opposite to that seen in the $i_{13/2}$ neutron bands and completely defy the simple explanation offered for the latter in terms of the particle-rotor model. The reason seems to be the fact that we now have an odd-proton instead of odd-neutron so that all the gyromagnetic factors are different. Also, $h_{9/2}$ is a $N = 5$ orbital whereas $i_{13/2}$ is a $N = 6$ orbital thus changing the sign of a part of the $B(M1)$ term. Significant rotational effects on $B(M1)$ values are also seen in the bands based on the $d_{5/2}$ and $h_{11/2}$ bands. Although the calculations are schematic in nature, since we have used them to

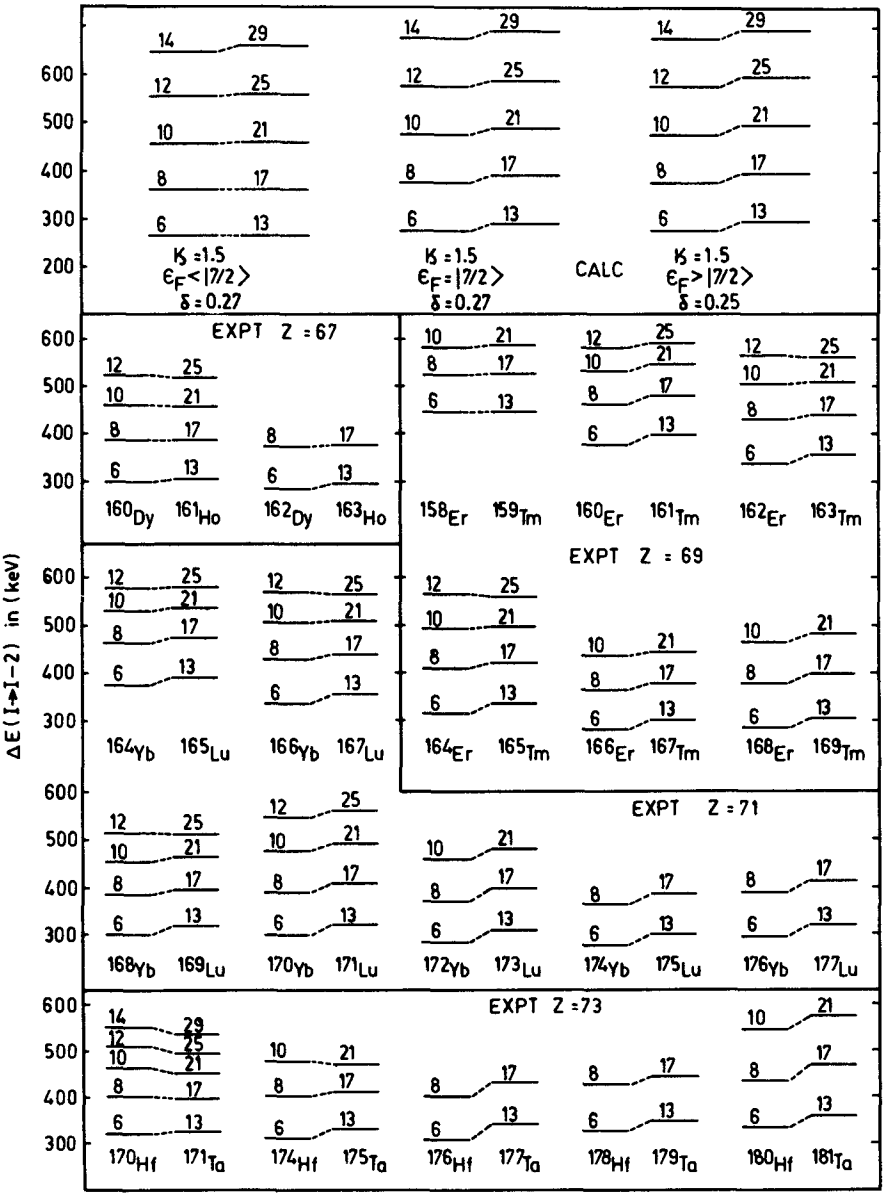

Figure 13. (a) Similar to figure 1 Here the Fermi energy is located near the $7/2^+[404]$ level of the $g_{7/2}$ orbital.

reproduce the characteristic decoupling patterns which we may take as signatures of a given nucleus, the subsequent calculations and effects are expected to be real and need to be verified by comparison with experimental data. Since not enough data is available to us we have refrained from making any systematic comparison. However, such a comparison will be highly useful in identifying any additional effects that must be included to explain any differing trends in the experimental data on transition probabilities.

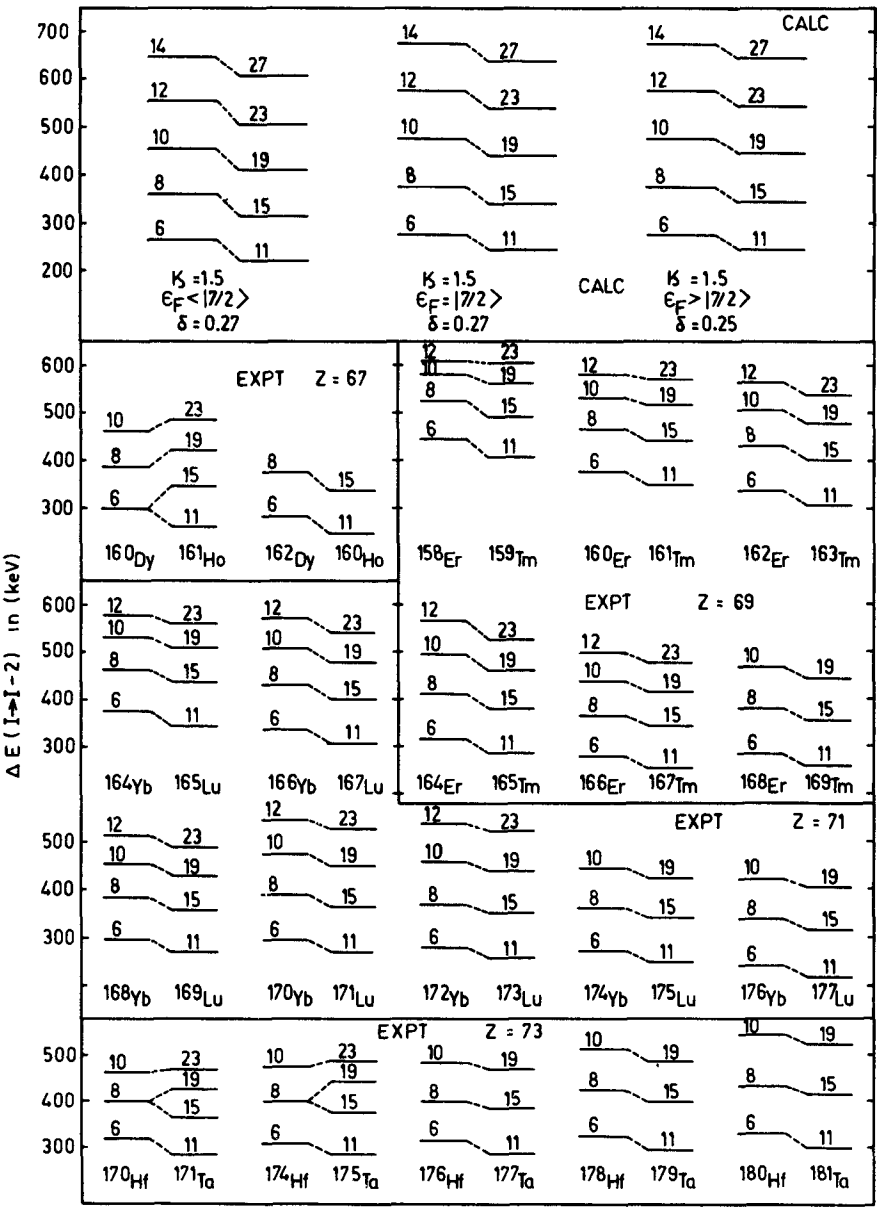

Figure 13. **(b)** Same as figure 13(a) but for the favoured sequence.

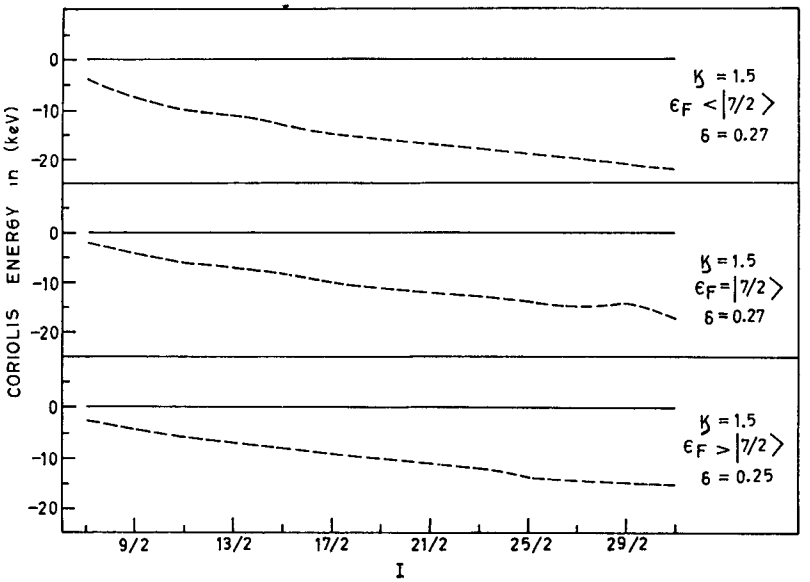

Figure 14. Similar to figure 2 but for the same sets of parameters as in figure 13.

Acknowledgements

Financial support from the Department of Atomic Energy, Government of India and the National Science Foundation under contract PHY-8605032 with Florida State University is acknowledged.

References

Bhattacharya S, Sen S and Guohhait R K 1985 *Phys. Rev.* **C32** 1026
Bohr A and Mottelson B R 1975 *Nuclear structure* (New York: Benjamin) Vol 2
Brockmeier R T, Wahlborn S, Seppi E J and Boehm F 1965 *Nucl. Phys.* **63** 102
Browne F and Femenia F R 1971 *Nucl. Data Tables* **10** 81
Bunker M F and Reich C W 1971 *Rev. Mod. Phys.* **43** 348
Chi B E 1966 *Nucl. Phys.* **83** 97
Engeland T, Henriquez A and Rekstad J 1983 *Phys. Lett.* **B120** 19
Hagemann G B, Garrett J D, Herskind B, Kownacki J, Nyako B M, Nolan P L, Sharpey-Schafer J F and Tjom P O 1984 *Nucl. Phys.* **A424** 365
Hamamoto I 1981 *Phys. Lett.* **B106** 281
Jain A K 1984 *Z. Phys.* **A317** 117
Jain K 1987 *New features in rotational bands of odd-A nuclei*, Ph.D. Thesis, University of Roorkee (unpublished)
Jain K and Jain A K 1984 *Phys Rev.* **C30** 2050
Jonsson S, Lyttkens J, Carlen L, Roy N, Ryde H, Walus W, Kownacki J, Hagemann G B, Herskind B, Garrett J D and Tjom P O 1984 *Nucl. Phys.* **A422** 397
Lamm I L 1969 *Nucl. Phys.* **A125** 504
Mosel U 1986 Invited talk at the Conference on Nuclear structure with heavy ions, Legnaro (Italy)
Muller E M and Mosel U 1984 *J. Phys.* **G10** 1523
Muller E M and Neergard K 1983 *Phys. Lett.* **B120** 280
Ogle W, Wahlborn S, Piepenbring R and Fredriksson S 1971 *Rev Mod Phys.* **43** 424
Popli R K, Grau J A, Popik S I, Samnelson L E, Rickey F A and Simms P C 1979 *Phys. Rev.* **C20** 1350
Rekstad J and Engeland T 1980 *Phys. Lett.* **B89** 316
Sakai M 1984 *At. Data Nucl. Data Tables* **31** 399

Smith H A Jr and Rickey F A 1979 *Phys. Rev* **C14** 1946
Stephens F S 1975 *Rev Mod Phys* **47** 43
Stephens F S, Diamond R M and Nilsson S G 1973 *Phys Lett.* **B44** 429
Stephens F S and Simon R S 1972 *Nucl Phys* **A183** 257
Table of Isotopes 1978 (eds) 7th edition C M Lederer and V S Shirley (New York: Wiley Interscience)
Wohn F K, Hill J C and Petry R F 1985 *Phys. Rev* **C31** 634
Zeghib S, Rickey F A and Simms P C 1986 *Phys Rev.* **C34** 1451